Am J Transl Res 2023;15(2):1072-1084
www.ajtr.org /ISSN:1943-8141/AJTR0146940

Original Article

RILPL2 is associated with the progression and prognosis of cervical squamous cell carcinoma and endocervical adenocarcinoma

Yanru Dong[1], Weibo Wen[1], Tiezheng Yuan[1], Lan Liu[2], Xiangdan Li[1]

[1]*Department of Morphological Experiment Center, Medical College of Yanbian University, Yanji 133000, Jilin, China;* [2]*Department of Pathology, Yanbian University Hospital, Yanji 133000, Jilin, China*

Received October 11, 2022; Accepted December 30, 2022; Epub February 15, 2023; Published February 28, 2023

Abstract: Cervical squamous cell carcinoma and endocervical adenocarcinoma (CESC) is one of the most common tumors among females worldwide. RILPL2 was recently reported to be a promising biomarker for the treatment of breast cancer. This study aimed to investigate the potential role of RILPL2 in CESC. Totally 302 CESC patients' data were downloaded from The Cancer Genome Atlas database. All patients were divided into high or low RILPL2 groups according to the median expression of RILPL2. Subsequently, survival analysis, multivariate Cox regression, and experimental validation were performed on all CESC patient data. The Ualcan database was used to analyze the expression level and prognostic value of RILPL2 in pan-cancer. The Gene Set Cancer Analysis database was used for drug sensitivity analysis. Functional KEGG pathways were analyzed using gene set enrichment analysis. RILPL2 was generally down-regulated in a variety of tumors, and a high level of RILPL2 was associated with a better prognosis in CESC patients. Immunohistochemistry, western blotting, and qRT-PCR results showed that RILPL2 was significantly down-regulated in CESC cells and tissues. Besides, along with the increase of TNM Stage, the RILPL2 expression tended to decrease gradually. Patients with high RILPL2 expression showed lower resistance to small molecule drugs used in CESC progressions, such as Methotrexate, AZD7762, and Vinblastine, and a higher response rate to immunotherapy. Additionally, we identified 267 co-expressing genes of RILPL2, all of which jointly affected CESC progression through 15 complex pathways. Low RILPL2 expression was closely associated with the onset, progression, and poor prognosis of CESC. RILPL2 might be a promising optional biomarker for CESC patients' diagnosis and prognosis.

Keywords: Cervical squamous cell carcinoma and endocervical adenocarcinoma (CESC), RILPL2, biomarker, prognosis, drug sensitivity

Introduction

Cervical squamous cell carcinoma and endocervical adenocarcinoma (CESC) is one of the most prevalent tumors among females worldwide [1], and it is the second most common type of gynecological cancer [2]. Annually, over 300,000 deaths result from CESC, about 85% of which occur in developing countries, according to a recent report [3]. Most CESC cases originate from persistent human papillomavirus (HPV) infection [4], and CESC progression is usually developed from a complex multistep process, including oncogenic HPV infection, squamous cervical intraepithelial lesion (CIN), carcinoma in situ to the expansion of carcinoma and invasion [5]. Despite the fact that several HPV vaccinations provide an essential prevention strategy for CESC, it is invalid in HPV-infected patients [4]. It is feasible to many CESC cases at this time by treating precancerous lesions at an early stage [4]. However, this is hard to achieve. Unfortunately, many CESC patients are diagnosed at an invasive stage, during which treatments are less effective than early interventions, and their prognoses are worse [6-8]. Consequently, early detection and timely diagnosis, in addition to necessary prevention, are the most effective approaches to improve the prognosis of CESC patients. Some previous studies attempted to find reliable novel biomarkers for CESC, for example, PDE2A

Table 1. Clinicopathological characteristics of cervical squamous cell carcinoma and endocervical adenocarcinoma (CESC)

Characteristics		Patients (283)	
		NO.	%
Age	≤ 46 (Median)	147	51.94%
	> 46 (Median)	136	48.06%
Grade	1	18	6.36%
	2	126	44.52%
	3	112	39.58%
	Unknown	27	9.54%
Pathologic stage	I	157	55.48%
	II	64	22.61%
	III	41	14.49%
	IV	21	7.42%
Survival time	Long (> 5 years)	41	14.49%
	Short (< 5 years)	242	85.51%
Overall survival status	Dead	70	24.73%
	Alive	213	75.27%

[9] and Klotho [1]. However, it is far from meeting CESC clinical requirements. Therefore, the continuous exploration of novel biomarkers would provide more options for early diagnosis of CESC.

Rab interacting lysosomal protein like 2 (RILPL2), also named RLP2, was initially found in ciliated mouse tracheal epithelial cells [10]. RILPL2 encodes a protein like Rab interacting lysosomal protein (RILP), and RILP has been indicated to serve as a tumor suppressor in lung cancer cells [11]. RILPL2 contains a conserved RILP homology domain, which is a Rab36 binding domain [12]. Inhibiting Rab36 expression was reported to be indirectly involved in suppressing bladder cancer [13]. Moreover, it has been suggested that RILPL2 was involved in hepatitis C virus (HCV) replication and could be a possible target for HCV treatment [14]. Besides, RILPL2 has been recently studied in breast cancer, and it has been demonstrated that low RILPL2 expression was observed in breast cancer tissues compared with adjacent tissues [15]. Not only that, RILPL2 could regulate the proliferation, metastasis, and chemoresistance of breast cancer via the TUBB3/PTEN pathway [15]. However, few other studies have focused on RILPL2 and cancer. To the extent of our knowledge, RILPL2 has never been systematically studied in CESC. Thus, we expected to find potential associations between RILPL2 and CESC to provide more reference information for further CESC exploration.

Herein, through a series of comprehensive analyses of mRNA expression data and clinical data of CESC patients downloaded from The Cancer Genome Atlas (TCGA) database, we aimed to evaluate the diagnostic and prognostic value of RILPL2 expression in CESC patients. Our research is expected to provide further insight into the possible mechanisms of RILPL2 in CESC and more options for biomarkers in the clinical treatment of CESC.

Materials and methods

Data acquisition

We downloaded the mRNA expression and clinical data of CESC patients from TCGA (https://tcga-data.nci.nih.gov/tcga/) database. Totally 302 CESC patient mRNA expression profiles and corresponding clinical data were obtained, which included 306 tumor tissues and 3 paired adjacent tissues. Moreover, 283 CESC patients with complete survival data were further analyzed. Additionally, all CESC patients were divided into a high RILPL2 expression group and a low RILPL2 expression group, according to the median expression of RILPL2. The detailed clinical data of 283 CESC patients were summarized in **Table 1**. We also downloaded the data of anti-PD-1 immunotherapy cohort GSE91061 (Illumina Genome Analyzer) from the GEO database, which contains 109 samples (51 pre-treatment samples and 56 post-treatment samples) for immunotherapy analysis.

Expression of RILPL2 in pan-cancer and its transcriptional regulation in cervical cancer samples

The Ualcan database (http://ualcan.path.uab.edu/) was used to analyze the expression of RILPL2 in pan-cancer [16]. The Cancer Cell Line Encyclopedia (CCLE, https://portals.broadinstitute.org/ccle) was utilized to verify the expression of RILPL2 in CESC cell lines. In addition, we used the Gene Set Cancer Analysis (GSCA) database (http://bioinfo.life.hust.edu.cn/GSCA) to explore the potential regulations for the low expression of the RILPL2 gene in

CESC, including DNA methylation, copy number variation (CNV), and target-regulatory miRNAs. GSCA has integrated the mRNA expression, mutation, immune infiltration, methylation data from TCGA database and the drug resistance data from Genomics of Drug Sensitivity in Cancer (GDSC) database (www.cancerRxgene.org).

Survival analysis

The overall survival (OS) of the high RILPL2 expression group and low RILPL2 expression group CESC patients was estimated by the survival package and survminer package (https://CRAN.R-project.org/package=survminer) in R software based on the Kaplan-Meier method. The log-rank test determined the significance of the OS difference between the two groups.

Gene set enrichment analysis (GSEA)

The GSEA analysis was performed after ranking according to the Fold Change value, which utilized GSEA (version: #4.0) software based on the gene set c2.cp.kegg.v7.0.symbols (as the preset functional gene subset) in the Molecular Signatures Database (MSigDB). The $P < 0.05$ was taken as the threshold to screen the significantly enriched KEGG pathways.

Immunohistochemical (IHC) method

For clinical validation, a cervical cancer tissue microarray (F541301, Zhongke Guanghua, Shanxi, China) was used in the present study, which contained 11 cervical squamous cell carcinoma specimens, 2 cervical adenosquamous carcinoma specimens, 5 cervical adenocarcinoma specimens, and the 18 corresponding adjacent normal specimens. Subsequently, the chip was combined with the primary antibody (Anti-RILPL2 antibody, ab153717, 1:500, Abcam, UK) and incubated overnight at 4°C. Then corresponding secondary antibody (cat#SE134, Solarbio, 1:150, Beijing, China) was added to the reaction system, incubating under room temperature for 35 min. Finally, the chip was stained for further observation.

Co-expressing genes network establishment of RILPL2 and functional enrichment analysis

Taking the expression matrix file as the input file, the co-expressing genes of RILPL2 in TCGA-CESC were screened by R software package (Psych and Hmisc). The correlation between RILPL2 expression level and co-expressing genes was screened by Pearson correlation coefficient (|Pearson correlation coefficient| > 0.5) and Z test ($P < 0.05$). The protein-protein interactions network (PPI) was constructed using the STRING database (v11.5, https://www.string-db.org/), which could identify the closely interactive proteins based on the experiment data, database data, gene adjacency, gene fusion, and gene co-expression. The clusterProfiler of R software was used for GO and KEGG pathways enrichment analysis. The $P < 0.05$ was applied to screen significantly enriched GO terms and KEGG pathways.

Significance of RILPL2 expression in drug therapy

We first used the GSCA database to perform drug sensitivity analysis on RILPL2 and the PPI network to identify the most closely interacting proteins of RILPL2. Then, we also used the GEO database PD-1 immunotherapy cohort GSE91061 to explore the relationship between RILPL2 expression and anti-PD-1 response rate and survival time.

Cell culture

Human cervical epithelial cell line H8 was purchased from Shanghai Baiye Biotechnology (Shanghai, China). Human cervical cancer cell lines, Hela and Ca Ski, were purchased from Wuhan University Cell Bank (Wuhan, China). Cell lines H8 and Ca Ski were cultured in RPMI-1640 medium (GIBCO, Cat#31800022). MEM medium (GIBCO, Cat#41500034) was used for Hela culture. All cells were cultured in 90% medium and 10% FBS at 37°C and 5% CO_2.

qRT-PCR

The TRIZOL reagent (Thermo, Cat#15596018, New York, USA) was used for total RNA extraction. The concentration and purity of the total RNA were measured by Nanodrop lite spectrophotometer (Thermo, New York, USA). Reverse transcription was conducted using a reverse transcription kit (Tiangen Biochemical, Cat#KR118, Beijing, China). Then qPCR was performed on a ROCHE fluorescent quantitative PCR machine with a SYBR detection kit (Tiangen, cat#FP205, Beijing, China). The pro-

cedure is as follows: 95°C, 15 min denaturation; 95°C, 10 sec; 60°C, 20 sec; 72°C, 20 sec; 40 cycles. The internal reference gene was β-actin. The primer: β-actin, Fwd: 5'-CCTGGCACCCAGCACAAT-3'; Rev: 5'-GGGCCGGACTCGTCATAC-3'; RILPL2, Fwd: 5'-CAAAATGGTGGTTGACCTGACA-3'; Rev: 5'-GGAGCTGCGACTTGAGT-3. Three wells were used for each sample. The mRNA expression level was calculated based on the formula $2^{-\Delta\Delta CT}$.

Western blot

Total protein was extracted from the cell lines. The BCA protein concentration detection kit (Solarbio, cat#PC0020, Beijing, China) and the ultra-micro spectrophotometer were used to determine the protein concentration and purity. The western blot method was consistent with the previous method [17]. The reagents used included the primary antibody Anti-RILPL2 antibody (ab153717, 1:1000, Abcam, UK), the internal reference GAPDH (cat#bs-2188R, 1:2000, Bioss, Beijing, China), and the secondary antibody IgG-HRP (cat#bs-0295G-HRP, 1:3000, Bioss, Beijing, China). The optical density analysis of all results was conducted via Gelpro32 software.

Statistical analysis

The differences in RILPL2 expression levels between tumor tissues and adjacent tissues and several other various clinicopathological characteristics were compared using the Wilcoxon rank sum test. Multivariate Cox regression proportional hazard model was used to determine the effect of RILPL2 expression and clinicopathological characteristics (Age, Grade, Stage, etc.) on the OS of CESC patients. A statistically significant difference was defined as $P < 0.05$. All statistical analyses were performed using R software (version v3.5.2).

Results

Low RILPL2 expression was associated with the occurrence of CESC

In the Ualcan database, we found that RILPL2 was lowly expressed in a variety of tumors but highly expressed in CHOL (cholangiocarcinoma), COAD (colon adenocarcinoma), ESCA (esophageal carcinoma), HNSC (head and neck squamous cancer), KIRC (kidney renal clear cell carcinoma), PCPG (pheochromocytoma and paraganglioma), SARC (sarcoma), and STAD (stomach adenocarcinoma), indicating that RILPL2 expression was tumor-specific (**Figure 1A**). In the survival analysis, RILPL2 was significantly associated with the prognosis of CESC, BRCA (breast cancer), HNSC, KIRC, LUAD (lung adenocarcinoma), SARC, SKCM (skin cutaneous melanoma), and UCEC (uterine corpus endometrial carcinoma), and high expression of RILPL2 indicated a better prognosis (**Figure 1B-I**). Furthermore, significantly lower RILPL2 expression was also observed in all CESC samples when compared to all adjacent normal tissues ($P = 0.0037$, **Figure 1J**). In the Cancer Cell Line Encyclopedia (CCLE) database, the expression of RILPL2 in the CESC cell line was notably lower than that in the normal cell line (**Figure 1K**). In addition, we also used IHC, western blot, and qRT-PCR to verify the abnormal reduction of RILPL2 expression in CESC tissues/cells (**Figures 1L**, S1 and **2A**, **2B**). Previous studies suggested that RILPL2 could inhibit breast cancer cell proliferation and migration by downregulating TUBB3 stability, suggesting that RILPL2 might be a suppressor regulating tumorigenesis [15]. In the present study, abnormally low expression of RILPL2 in CESC tissues might contribute to tumorigenesis, and the lower the expression of RILPL2, the worse the prognosis of patients.

The expression of RILPL2 might be regulated by hsa-miR-1237

Our above study suggested that the expression of RILPL2 was down-regulated in CESC. To further explore the underlying cause of RILPL2 down-regulation, we used the TCGA-CESC dataset in the GSCA database to analyze the relationship between RILPL2 expression and methylation, CNV and target-regulatory miRNAs. As shown in **Figure 2C**, the mutation rate of RILPL2 was low, and the correlation between RILPL2 expression level and CNV was extremely weak (**Figure 2D**). Then we analyzed the relationship between RILPL2 expression and methylation levels. The results showed that RILPL2 only had a weak negative correlation with cg04781075 ($R = -0.19$, **Figure 2E**). The methylation level of RILPL2 was not associated with disease-free interval (DFI), disease-specific survival (DSS), progression-free survival

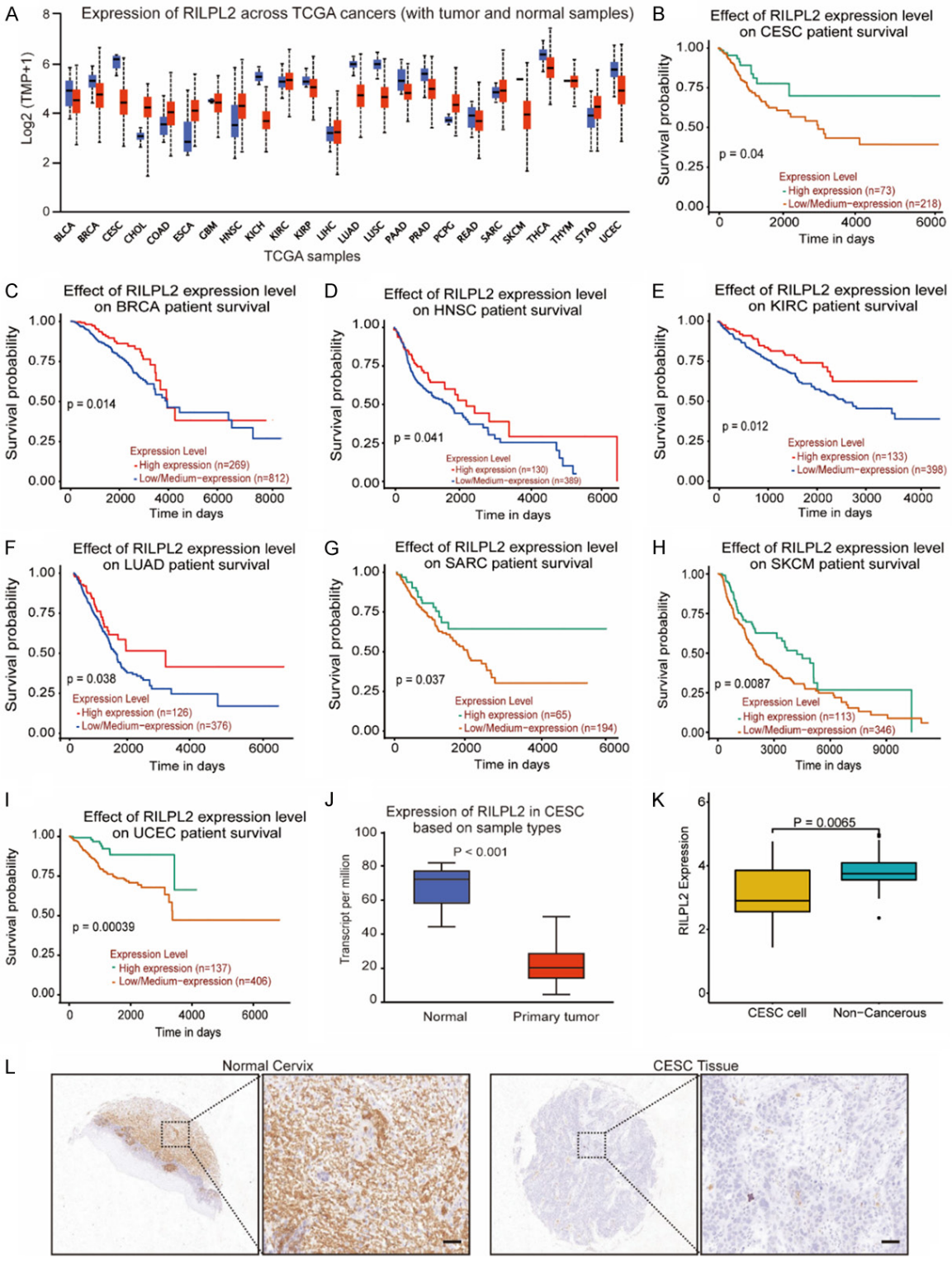

Figure 1. Expression of RILPL2 in pan-cancer and its prognostic value for cervical squamous cell carcinoma and endocervical adenocarcinoma (CESC). A. Expression levels of RILPL2 in 24 types of cancer. B-I. High expression of RILPL2 was associated with a better prognosis for CESC, BRCA (breast cancer), HNSC (head and neck squamous cancer), KIRC (kidney renal clear cell carcinoma), LUAD (lung adenocarcinoma), SARC (sarcoma), SKCM (skin cutaneous melanoma), and UCEC (uterine corpus endometrial carcinoma) patients, respectively. J. RILPL2 was significantly down-regulated in CESC in the TGCA database. K. RILPL2 was significantly down-regulated in CESC cell lines in the Cancer Cell Line Encyclopedia (CCLE) database. L. Immunohistochemistry representation of RILPL2 expression in normal cervix and CESC tissue. Scale bar = 50 μm.

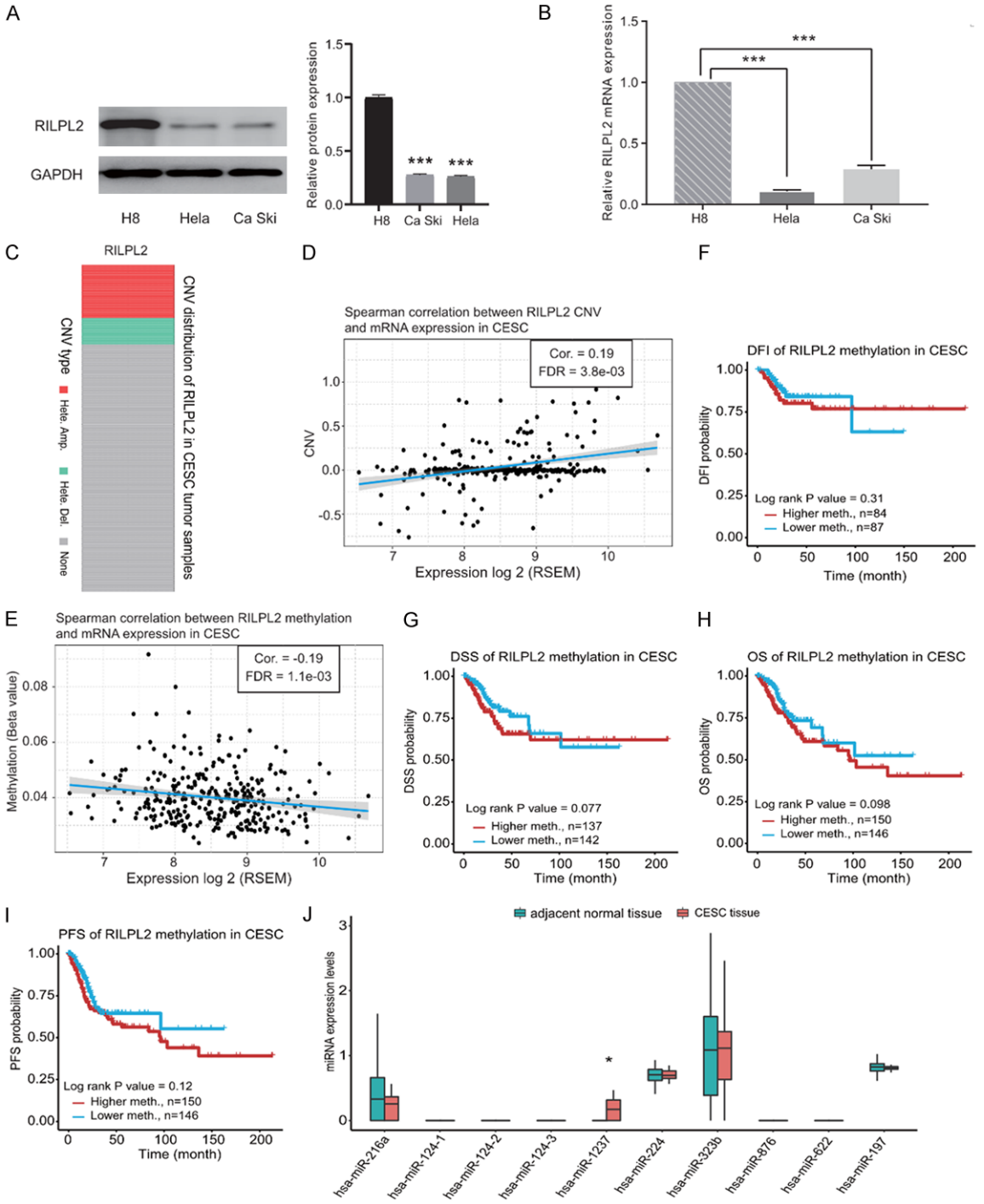

Figure 2. Exploration of CNV level, methylation level, and target-regulatory miRNAs of RILPL2. A, B. The expression of RILPL2 in the CESC cell lines Hela and Ca Ski was determined by western blot and qRT-PCR. ***P < 0.001 vs. H8 group. C. Histogram of RILPL2 CNV mutations. D. Correlation between RILPL2 mRNA expression and CNV. E. Correlation between RILPL2 mRNA expression and methylation. F-I. There was no significant difference in the survival curves of DFI, DSS, OS, and PFS between CESC patients with high and low methylation levels of RILPL2. J. The expression level of target-regulatory miRNAs of RILPL2.

(PRS), and OS (**Figure 2F-I**). In addition, we predicted several miRNAs that regulate RILPL2 expression, including hsa-miR-216a, hsa-miR-124-1, hsa-miR-124-2, hsa-miR-124-3,

hsa-miR-1237, hsa-miR-224, hsa-miR-323b, hsa-miR-876, hsa-miR-622, and hsa-miR-197 (Figure S2). Notably, we found that the target-regulatory miRNA of RILPL2, hsa-miR-1237 (**Figure 2J**), was highly expressed in CESC, suggesting that the high expression of hsa-miR-1237 might down-regulate the expression of RILPL2 in CESC tissue.

The association between RILPL2 expression with stage, grade, and age of CESC patients

The association between RILPL2 mRNA expression and several clinicopathological characteristics of CESC patients was determined using the Wilcoxon rank sum test. The results indicated that with the increase of TNM stage, the expression level of RILPL2 gradually decreased, and there were significant statistical differences in Stage I vs. Stage II, Stage I vs. Stage III, and Stage I vs. Stage IV ($P < 0.05$, **Figure 3A**). However, there was no significant difference in RILPL2 expression in CESC patients of different grades or ages ($P > 0.05$, **Figure 3B**, **3C**). To determine whether RILPL2 was an independent prognostic indicator, we included age, grade, stage, and RILPL2 in a multivariate Cox regression analysis. The results showed that RILPL2 expression was still significantly associated with OS, and samples with low RILPL2 expression had a higher risk of death (HR = 0.74, 95% CI: 0.56-0.99, P = 0.045) (**Figure 3D**).

The GSEA results based on the RILPL2 expression

As mentioned above, high expression of RILPL2 was associated with better prognosis, suggesting that RILPL2 might be involved in inhibiting tumor progression. To further understand the potential tumor suppressor mechanism of RILPL2, we divided the patients in the TCGA-CESC cohort into the high RILPL2 expression group and the low RILPL2 expression group according to the median RILPL2 expression. Then GSEA enrichment analysis was used to identify significantly activated signaling pathways between the two groups. We found that compared with the low RILPL2 expression group, there were a total of 17 KEGG pathways significantly activated in the high RILPL2 expression group, such as CELL_ADHESION_MOLECULES_CAMS, ALDOSTERONE_REGULATED_SODIUM_REABSORPTION. Among these, the most significant 5 pathways were displayed in **Figure 3E-I**, and the detailed information of 17 pathways was listed in Table S1. These activated pathways indicated that the effects of RILPL2 on tumor progression were multi-faceted and multi-pathways.

Co-expressing genes network establishment for RILPL2

To further investigate the genes closely related to RILPL2 in CESC, R software packages (Psych and Hmisc) were used to screen RILPL2 co-expressed genes in TCGA-CESC. Subsequently, a total of 267 related genes were screened (Table S2). Then, we constructed a PPI network for RILPL2 and 267 genes. Of note, the results showed that RILPL2 had the strongest interaction with RAB36, TCTN2, TCTN1, TCTN3, VPS33A, ARL1, COG7, SYS1, B9D2, and BBS12 (**Figure 4A**). Moreover, KEGG and GO enrichment analyses were performed on these co-expressed genes. KEGG enrichment analysis indicated that 15 pathways were significantly activated, including lysosome, leukocyte transendothelial migration, cytokine-cytokine receptor interaction, and cell adhesion molecules (**Figure 4B**). GO analysis showed that 31 biological processes were significantly activated, including cytokine binding, guanyl ribonucleotide binding, guanyl nucleotide binding, and GTP binding (**Figure 4C**).

High expression of RILPL2 might have a higher response rate to drug therapy

Whether the expression of RILPL2 could indicate the choice of drug therapy for patients was of interest to us. Therefore, we performed a drug sensitivity analysis on RILPL2 using the GSCA database. We found that RILPL2 was negatively correlated with most drugs (such as Methotrexate, AZD7762, and Vinblastine, **Figure 5A**), indicating that high expression of PILPL2 was not the cause of resistance to these drugs. However, publicly available datasets of CESC patients receiving immunotherapy were lacking. Therefore, a dataset of malignant melanomas treated with anti-PD-1 and anti-CTLA4 (GSE91016) was used to assess the rate of response of high RILPL2 expression to anti-PD-1 [18]. The results showed that the ratio of partial response/complete response (PR/CR) in the low RILPL2 expression group was 7.14% and that in the high RILPL2 expres-

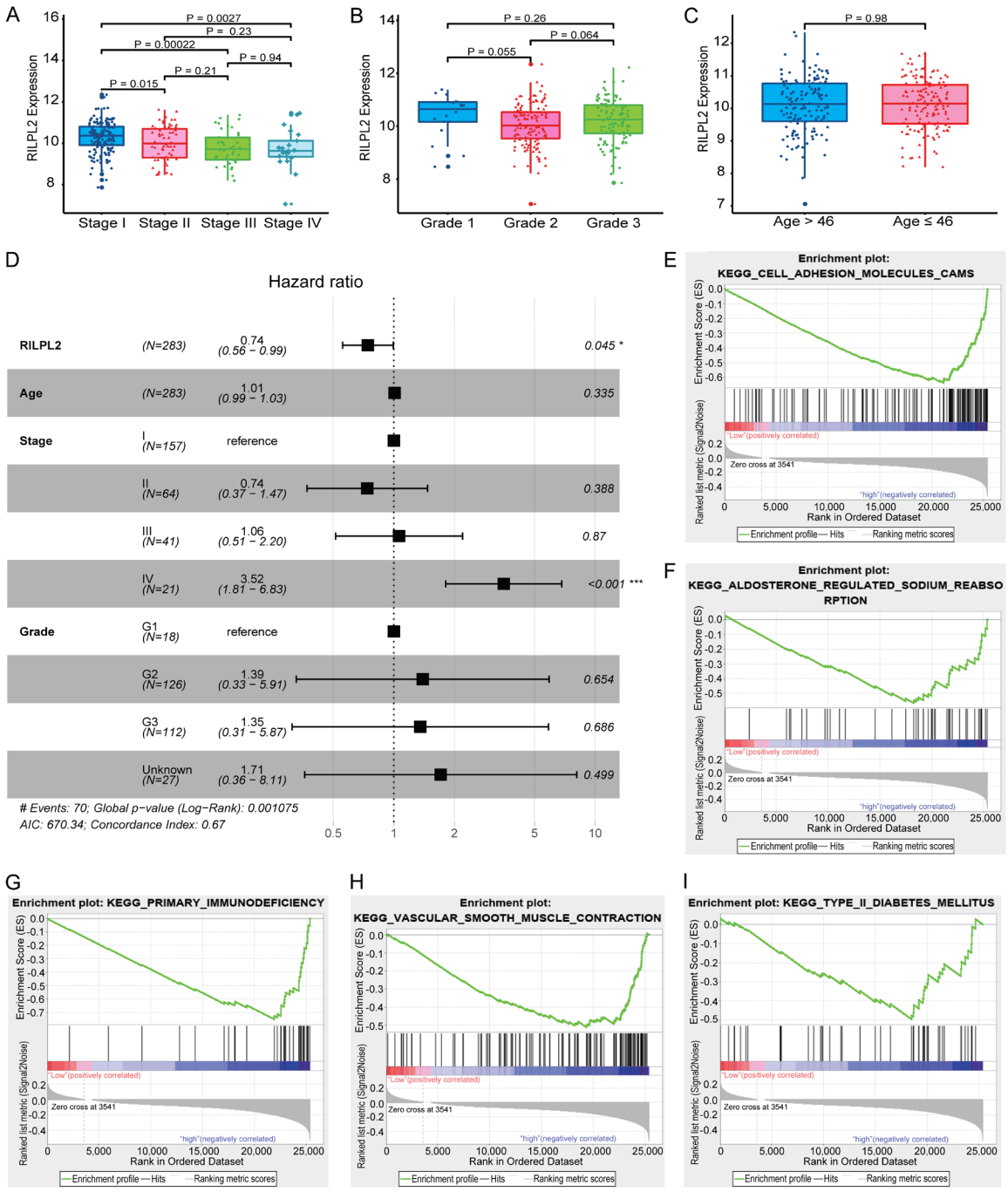

Figure 3. Relationship between RILPL2 and clinicopathological features. A. The expression level of RILPL2 at different TNM stages. B. The expression level of RILPL2 at different grades. C. The expression level of RILPL2 at different ages. D. In the multivariate Cox regression analysis forest map, the sample with a Hazard ratio greater than 1 had a higher risk of death, and the sample with a Hazard ratio less than 1 had a lower risk of death. E-I. The GSEA results based on RILPL2 expression.

sion group was 39.29%, indicating that the high RILPL2 expression group had a higher response rate to anti-PD-1 treatment (chi-square test P = 0.01134, **Figure 5B**).

Discussion

As far as we know, this is the first study on the role of RILPL2 in CESC. In the present study,

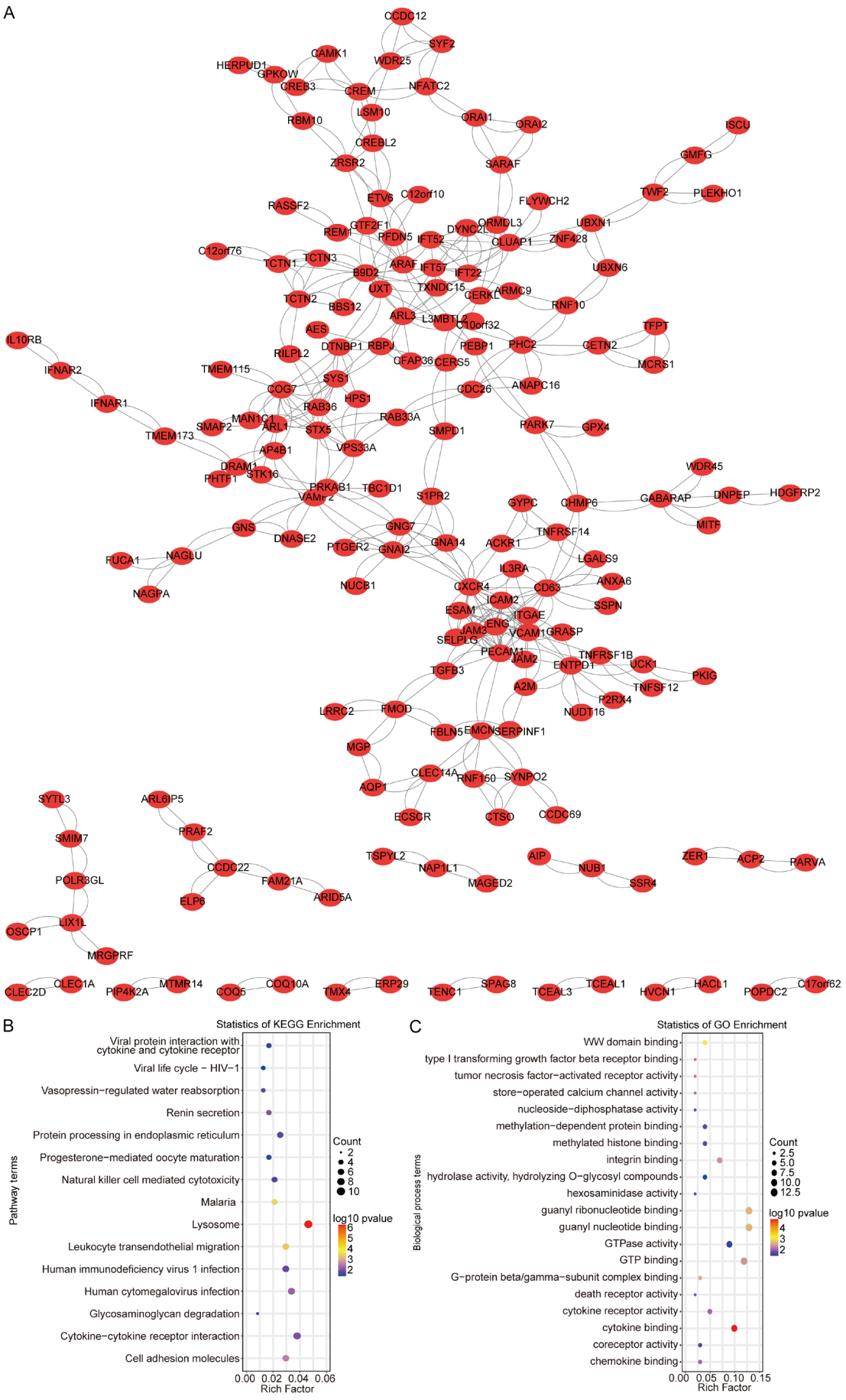
A
CCDC12
SYF2
CAMK1
WDR25
HERPUD1
GPKOW
CREB3
CREM
NFATC2
LSM10
RBM10
ORAI1
ORAI2
ISCU
CREBL2
GMFG
ZRSR2
SARAF
ETV6
C12orf10
TWF2
PLEKHO1
RASSF2
FLYWCH2
GTF2F1
REM1
PFDN5
IFT52
DYNC2L
ORMDL3
UBXN1
CLUAP1
ZNF428
C12orf76
TCTN1
TCTN3
ARAF
IFT57
IFT22
B9D2
UBXN6
UXT
TXNDC15
CERKL
ARMC9
TCTN2
BBS12
RNF10
ARL3
L3MBTL2
C10orf32
AES
TFPT
IL10RB
DTNBP1
RBPJ
PEBP1
PHC2
CETN2
RILPL2
CFAP36
CERS5
MCRS1
IFNAR2
TMEM115
SYS1
CDC26
ANAPC16
COG7
IFNAR1
HPS1
RAB36
MAN1C1
RAB33A
SMAP2
ARL1
STX5
SMPD1
PARK7
GPX4
TMEM173
AP4B1
VPS33A
DRAM1
RHTF1
STK16
WDR45
PRKAB1
TBC1D1
S1PR2
GABARAP
DNPEP
HDGFRP2
VAMP2
GYPC
CHMP6
MITF
GNS
GNG7
TNFRSF14
DNASE2
PTGER2
GNAI2
GNA14
ACKR1
FUCA1
NAGLU
LGALS9
IL3RA
NUCB1
CXCR4
CD63
ANXA6
NAGPA
ICAM2
SSPN
ESAM
ITGAE
ENG
JAM3
VCAM1
GRASP
SELPLG
PECAM1
TNFRSF1B
JAM2
ENTPD1
UCK1
TGFB3
PKIG
A2M
TNFSF12
P2RX4
LRRC2
FMOD
NUDT16
FBLN5
EMCN
SERPINF1
MGP
CLEC14A
AQP1
RNF150
SYNPO2
ECSCR
CTSC
CCDC69
SYTL3
ARL6IP5
SMIM7
PRAF2
CCDC22
TSPYL2
NAP1L1
AIP
NUB1
ZER1
ACP2
PARVA
POLR3GL
FAM21A
MAGED2
SSR4
ELP6
ARID5A
OSCP1
LIX1L
MRGPRF
CLEC2D
CLEC1A
PIP4K2A
MTMR14
COQ5
COQ10A
TMX4
ERP29
TENC1
SPAG8
TCEAL3
TCEAL1
HVCN1
HACL1
POPDC2
C17orf62
B
Statistics of KEGG Enrichment
Viral protein interaction with cytokine and cytokine receptor
Viral life cycle − HIV−1
Vasopressin−regulated water reabsorption
Renin secretion
Protein processing in endoplasmic reticulum
Progesterone−mediated oocyte maturation
Natural killer cell mediated cytotoxicity
Malaria
Lysosome
Leukocyte transendothelial migration
Human immunodeficiency virus 1 infection
Human cytomegalovirus infection
Glycosaminoglycan degradation
Cytokine−cytokine receptor interaction
Cell adhesion molecules
Pathway terms
0.00 0.02 0.04 0.06
Rich Factor
Count
2
4
6
8
10
log10 pvalue
6
5
4
3
2
C
Statistics of GO Enrichment
WW domain binding
type I transforming growth factor beta receptor binding
tumor necrosis factor−activated receptor activity
store−operated calcium channel activity
nucleoside−diphosphatase activity
methylation−dependent protein binding
methylated histone binding
integrin binding
hydrolase activity, hydrolyzing O−glycosyl compounds
hexosaminidase activity
guanyl ribonucleotide binding
guanyl nucleotide binding
GTPase activity
GTP binding
G−protein beta/gamma−subunit complex binding
death receptor activity
cytokine receptor activity
cytokine binding
coreceptor activity
chemokine binding
Biological process terms
0.00 0.05 0.10 0.15
Rich Factor
Count
2.5
5.0
7.5
10.0
12.5
log10 pvalue
4
3
2

Figure 4. Co-expressing genes network establishment of RILPL2 and functional enrichment analysis. A. The PPI network of RILPL2 and 267 co-expressing genes. B, C. The results of KEGG pathway analysis and GO analysis.

we downloaded the public CESC patient data from the TCGA database, and further analysis and experimental validation were conducted. Subsequently, we found that low RILPL2 expression was closely correlated with the occurrence of CESC. In addition, we found that compared with patients with high RILPL2 expression, CESC patients with low RILPL2 expression had a poorer prognosis.

As early detection showed a crucial effect on the prognosis of CESC patients, significant efforts have been devoted to exploring novel biomarkers for CESC [19, 20]. First, the RILPL2 expression levels in CESC tissues and adjacent tissues were compared to confirm whether RILPL2 was related to the occurrence of CESC. Subsequently, compared with adjacent tissues, there was a significantly lower RILPL2 expression in CESC tissues, which indicated that low RILPL2 expression was closely correlated with the occurrence of CESC. Our results were consistent with previous similar research in breast cancer. There was lower RILPL2 expression in breast cancer tissues than that in adjacent tissues [15]. Additionally, the association between RILPL2 expression and the clinicopathological characteristics of CESC was also investigated. Along with the increase in TNM stage, RILPL2 expression tended to decrease gradually. This finding reminded us that decreased RILPL2 expression probably influenced the proliferation, migration, and invasion of CESC cells, either directly or indirectly [21, 22]. However, the exact mechanism should be further explored in the future.

Better prognosis has been the ultimate aim of CESC research, and earlier diagnosis is a practical way to realize it [23]. Based on the results of survival analysis and multivariate Cox regression analysis, RILPL2 expression was an independent prognostic indicator of CESC. CESC patients with low RILPL2 expression had a poorer prognosis than high RILPL2 expression ones, implying that RILPL2 might be a potential prognostic biomarker for CESC. RILPL2 encodes a protein like Rab interacting lysosomal protein (RILP), and RILP has been indicated to serve as a tumor suppressor in lung cancer cells [11]. In a recent breast cancer study, RILPL2 was reported to be a tumor suppressor in breast cancer as RILPL2 overexpression inhibited breast cancer cell proliferation and metastasis [15]. However, the study did not clarify the direct relationship between the RILPL2 and the prognosis of breast cancer prognosis. At this point, we have first demonstrated the association between RILPL2 expression and the prognosis of CESC.

To lay the foundation for further exploration of the role of RILPL2 in CESC, the significantly differential functional KEGG pathways between high and low RILPL2 expression CESC patients were also enriched in our study. A total of 17 differential KEGG pathways were found, including Cell Adhesion Molecules (CAM) and Aldosterone Regulated Sodium Reabsorption. Regarding the CAM pathway, the pivotal role of CAM in the development of various tumors has been widely reported, for instance, in recurrent and distant metastasis of cancer [24]. De Méndez et al. documented that three CAMs (E-cadherin, CD44s, and CD44v3) significantly differed in cervical cancer and normal tissues. These CAMs could be potential biomarkers for invasive cervical neoplasia [25]. Furthermore, we noticed that several distinct pathways were associated with the immune response, including primary immunodeficiency [26], leukocyte transendothelial migration [27], systemic lupus erythematosus [28], and complement and coagulation cascades [29, 30], most of which were evidenced to be significantly responsible for CESE or other cancers. Collectively, although the exact mechanisms behind RILPL2 in CESC are not evident in the present research, we will further investigate the role of RILPL2 in CESC based on the results of differential functional KEGG pathways.

In addition, the study also investigated the relationship between the expression level of RILPL2 and drug treatment. The results suggested that RILPL2 expression was negatively correlated with a variety of small molecule drugs, which indicated that patients with high RILPL2 expression might have a lower probability of resistance to these drugs and more significant benefit from the treatment. Due to the lack of publicly available immunotherapy datasets for

Figure 5. Analysis of drug sensitivity and anti-PD-1 treatment response. A. Drug sensitivity analysis of RILPL2 and its highly related co-expressing genes based on GDSC database. B. The CR/PR response rate difference between the high RILPL2 expression group and the low RILPL2 expression group to anti-PD-1 treatment.

CESC patients, we used immunotherapy data from melanoma patients to analyze the differences in CR/PR between high-and low-expression subgroups defined based on RILPL2 levels. As we mentioned above, patients in the high-expression group had a higher CR/PR ratio. These data provided a reference for drug selection for the clinical treatment of CESC patients. However, our findings have yet to be validated in clinical trials, which will be the focus of our future research.

Conclusions

In summary, our study, for the first time, explored the potential role of RILPL2 expression in CESC based on a series of comprehensive analyses of CESC patient data and further validation experiments. Our findings indicated that low RILPL2 expression was closely associated with the onset, progression, and poor prognosis of CESC. RILPL2 might be a promising optional biomarker for CESC patients' diagnosis and prognosis.

Disclosure of conflict of interest

None.

Address correspondence to: Dr. Xiangdan Li, Department of Morphological Experiment Center, Medical College of Yanbian University, No. 977, Gongyuan Road, Yanji 133000, Jilin, China. Tel: +86-0433-2435113; E-mail: lixiangdan@ybu.edu.cn; Dr. Lan Liu, Department of Pathology, Yanbian University Hospital, No. 1327, Juzi Street, Yanji 133000, Jilin, China. Tel: +86-0433-2660121; E-mail: lliu@ybu.edu.cn

References

[1] Aviel-Ronen S, Rubinek T, Zadok O, Vituri A, Avivi C, Wolf I and Barshack I. Klotho expression in cervical cancer: differential expression in adenocarcinoma and squamous cell carcinoma. J Clin Pathol 2016; 69: 53-57.

[2] Koh WJ, Abu-Rustum NR, Bean S, Bradley K, Campos SM, Cho KR, Chon HS, Chu C, Clark R, Cohn D, Crispens MA, Damast S, Dorigo O, Eifel PJ, Fisher CM, Frederick P, Gaffney DK, Han E, Huh WK, Lurain JR, Mariani A, Mutch D, Nagel C, Nekhlyudov L, Fader AN, Remmenga SW, Reynolds RK, Tillmanns T, Ueda S, Wyse E, Yashar CM, McMillian NR and Scavone JL. Cervical cancer, version 3.2019, NCCN clinical practice guidelines in oncology. J Natl Compr Canc Netw 2019; 17: 64-84.

[3] Bray F, Ferlay J, Soerjomataram I, Siegel RL, Torre LA and Jemal A. Global cancer statistics 2018: GLOBOCAN estimates of incidence and mortality worldwide for 36 cancers in 185 countries. CA Cancer J Clin 2018; 68: 394-424.

[4] Ayen A, Jimenez Martinez Y and Boulaiz H. Targeted gene delivery therapies for cervical cancer. Cancers (Basel) 2020; 12: 1301.

[5] Woodman CB, Collins SI and Young LS. The natural history of cervical HPV infection: unresolved issues. Nat Rev Cancer 2007; 7: 11-22.

[6] Chesson HW, Blandford JM, Gift TL, Tao G and Irwin KL. The estimated direct medical cost of sexually transmitted diseases among American youth, 2000. Perspect Sex Reprod Health 2004; 36: 11-19.

[7] Subramanian S, Trogdon J, Ekwueme DU, Gardner JG, Whitmire JT and Rao C. Cost of cervical cancer treatment: implications for providing coverage to low-income women under the Medicaid expansion for cancer care. Womens Health Issues 2010; 20: 400-405.

[8] Lahue BJ, Baginska E, Li SS and Parisi M. Health technology assessment on cervical cancer screening, 2000-2014. Int J Technol Assess Health Care 2015; 31: 171-180.

[9] Ding H, Xiong XX, Fan GL, Yi YX, Chen YR, Wang JT and Zhang W. The new biomarker for cervical squamous cell carcinoma and endocervical adenocarcinoma (CESC) based on public database mining. Biomed Res Int 2020; 2020: 5478574.

[10] Schaub JR and Stearns T. The Rilp-like proteins Rilpl1 and Rilpl2 regulate ciliary membrane content. Mol Biol Cell 2013; 24: 453-464.

[11] Lin J, Zhuo Y, Yin Y, Qiu L, Li X and Lai F. Methylation of RILP in lung cancer promotes tumor cell proliferation and invasion. Mol Cell Biochem 2021; 476: 853-861.

[12] Matsui T, Ohbayashi N and Fukuda M. The Rab interacting lysosomal protein (RILP) homology domain functions as a novel effector domain for small GTPase Rab36: Rab36 regulates retrograde melanosome transport in melanocytes. J Biol Chem 2012; 287: 28619-28631.

[13] Zhu Y, Liang S, Pan H, Cheng Z and Rui X. Inhibition of miR-1247 on cell proliferation and invasion in bladder cancer through its downstream target of RAB36. J Biosci 2018; 43: 365-373.

[14] Dolan PT, Zhang C, Khadka S, Arumugaswami V, Vangeloff AD, Heaton NS, Sahasrabudhe S, Randall G, Sun R and LaCount DJ. Identification and comparative analysis of hepatitis C virus-host cell protein interactions. Mol Biosyst 2013; 9: 3199-3209.

[15] Chen G, Sun L, Han J, Shi S, Dai Y and Liu W. RILPL2 regulates breast cancer proliferation,

metastasis, and chemoresistance via the TUBB3/PTEN pathway. Am J Cancer Res 2019; 9: 1583-1606.
[16] Xu M, Xu J, Zhu D, Su R, Zhuang B, Xu R, Li L, Chen S and Ling Y. Expression and prognostic roles of PRDXs gene family in hepatocellular carcinoma. J Transl Med 2021; 19: 126.
[17] Wang YX, Liu L, Zeng QX, Fan TY, Jiang JD, Deng HB and Song DQ. Synthesis and identification of novel berberine derivatives as potent inhibitors against TNF-alpha-induced NF-kappaB activation. Molecules 2017; 22: 1257.
[18] Wang S, Xiong Y, Zhang Q, Su D, Yu C, Cao Y, Pan Y, Lu Q, Zuo Y and Yang L. Clinical significance and immunogenomic landscape analyses of the immune cell signature based prognostic model for patients with breast cancer. Brief Bioinform 2021; 22: bbaa311.
[19] Chaichian S, Shafabakhsh R, Mirhashemi SM, Moazzami B and Asemi Z. Circular RNAs: a novel biomarker for cervical cancer. J Cell Physiol 2020; 235: 718-724.
[20] Ye H and Guo X. TP73 is a credible biomarker for predicting clinical progression and prognosis in cervical cancer patients. Biosci Rep 2019; 39: BSR20190095.
[21] Song T, Xu A, Zhang Z, Gao F, Zhao L, Chen X, Gao J and Kong X. CircRNA hsa_circRNA_101996 increases cervical cancer proliferation and invasion through activating TPX2 expression by restraining miR-8075. J Cell Physiol 2019; 234: 14296-14305.
[22] Chiang AJ, Li CJ, Tsui KH, Chang C, Chang YI, Chen LW, Chang TH and Sheu JJ. UBE2C drives human cervical cancer progression and is positively modulated by mTOR. Biomolecules 2020; 11: 37.
[23] Meng H, Liu J, Qiu J, Nie S, Jiang Y, Wan Y and Cheng W. Identification of key genes in association with progression and prognosis in cervical squamous cell carcinoma. DNA Cell Biol 2020; 39: 848-863.
[24] Okegawa T, Pong RC, Li Y and Hsieh JT. The role of cell adhesion molecule in cancer progression and its application in cancer therapy. Acta Biochim Pol 2004; 51: 445-457.
[25] de Mendez MT and Bosch AL. Abnormal immunoexpression of cell adhesion molecules (CAMs) in cervical cancer. Int J Surg Pathol 2011; 19: 733-742.
[26] Kebudi R, Kiykim A and Sahin MK. Primary immunodeficiency and cancer in children; a review of the literature. Curr Pediatr Rev 2019; 15: 245-250.
[27] Jin GH, Xu W, Shi Y and Wang LB. Celecoxib exhibits an anti-gastric cancer effect by targeting focal adhesion and leukocyte transendothelial migration-associated genes. Oncol Lett 2016; 12: 2345-2350.
[28] Bruera S, Lei X, Zogala R, Pundole X, Zhao H, Giordano SH, Hwang JP, Rauh-Hain JA and Suarez-Almazor ME. Cervical cancer screening in women with systemic lupus erythematosus. Arthritis Care Res (Hoboken) 2021; 73: 1796-1803.
[29] Zhang J, Chen M, Zhao Y, Xiong H, Sneh T, Fan Y, Wang J, Zhou X and Gong C. Complement and coagulation cascades pathway correlates with chemosensitivity and overall survival in patients with soft tissue sarcoma. Eur J Pharmacol 2020; 879: 173121.
[30] Liu Y, Xiong S, Liu S, Chen J, Yang H, Liu G and Li G. Analysis of gene expression in bladder cancer: possible involvement of mitosis and complement and coagulation cascades signaling pathway. J Comput Biol 2020; 27: 987-998.

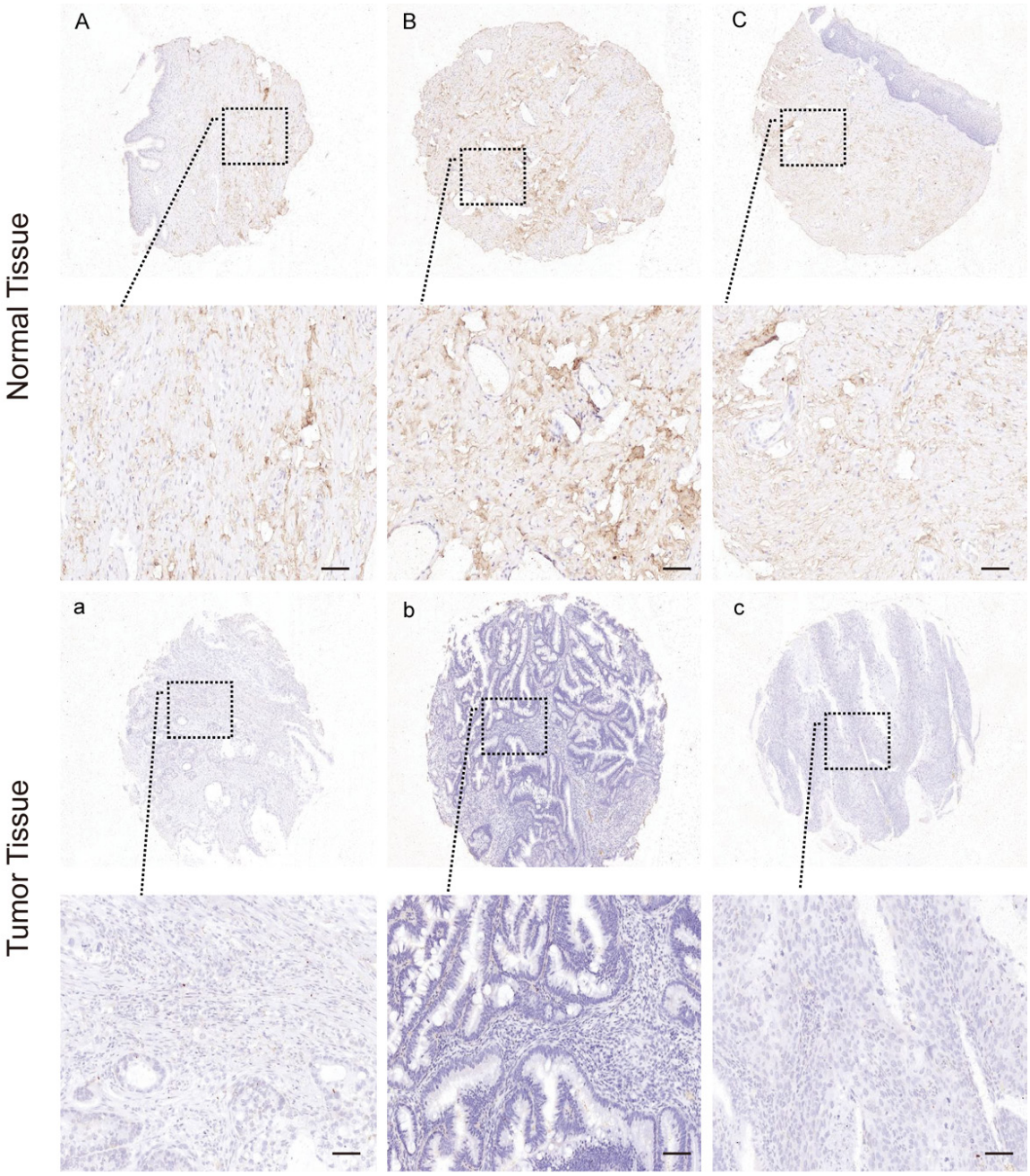

Figure S1. IHC of RILPL2 expression in normal cervix and CESC tissue. Scale bar = 50 μm.

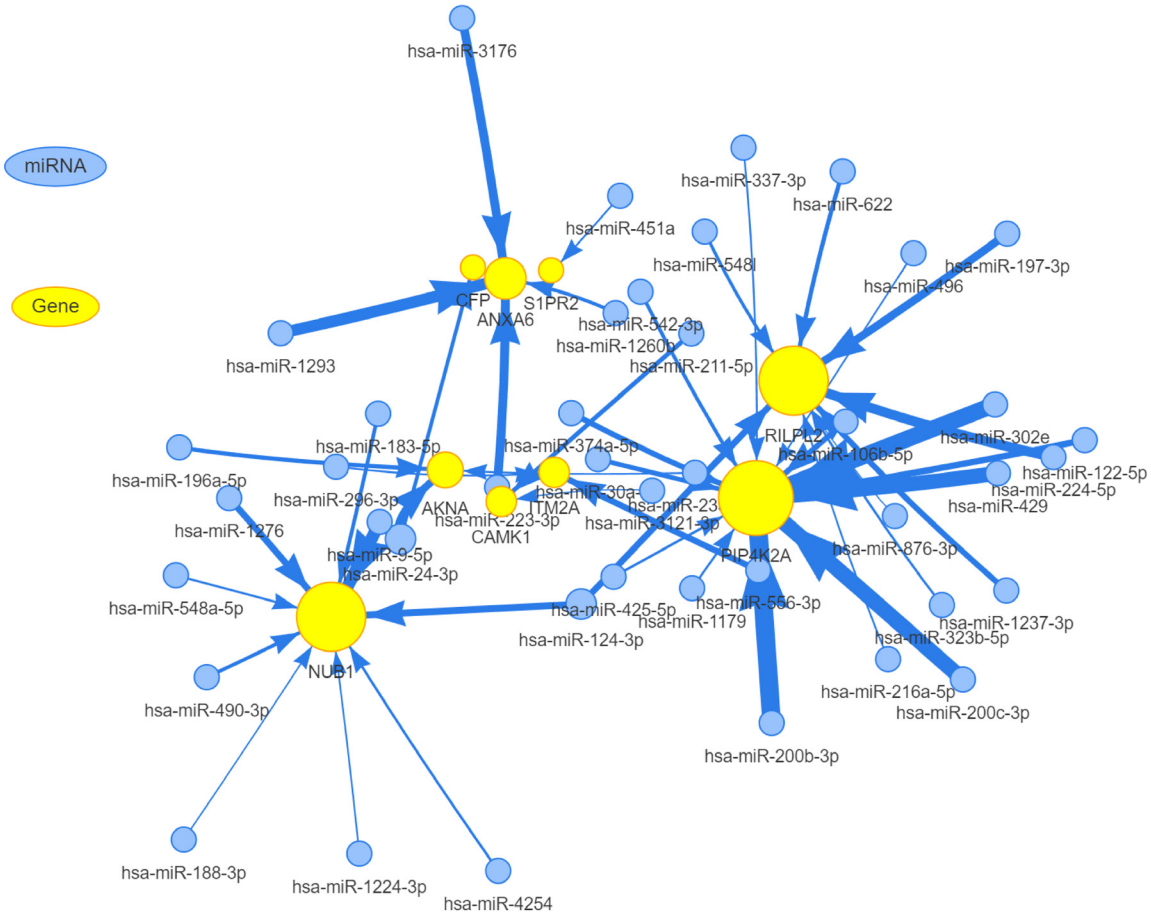

Figure S2. Interaction network between RILPL2 and its target-regulatory miRNAs. The expression of RILPL2 might be regulated by hsa-miR-1237.